01 Jan 2007

Heat Transfer Coefficients in a High-Pressure Bubble Column

Chengtian Wu

Muthanna H. Al-Dahhan
Missouri University of Science and Technology, aldahhanm@mst.edu

Anand Prakash

Recommended Citation

C. Wu et al., "Heat Transfer Coefficients in a High-Pressure Bubble Column," *Chemical Engineering Science*, vol. 62, no. 1 thru 2, pp. 140 - 147, Elsevier, Jan 2007.
The definitive version is available at https://doi.org/10.1016/j.ces.2006.08.016

ELSEVIER

Chemical Engineering Science 62 (2007) 140–147

Chemical Engineering Science

www.elsevier.com/locate/ces

Heat transfer coefficients in a high-pressure bubble column

Chengtian Wu[a], Muthanna H. Al-Dahhan[a,*], Anand Prakash[b]

[a]*Chemical Reaction Engineering Laboratory, Department of Chemical Engineering, Washington University in St. Louis, St. Louis, MO 63130, USA*
[b]*Department of Chemical and Biochemical Engineering, University of Western Ontario, London, Ont., Canada N6A 5B9*

Available online 23 August 2006

Abstract

Time-averaged local heat transfer coefficients were studied in a 0.16 m inner diameter high-pressure air–water bubble column. The effects of the superficial gas velocity (up to 0.30 m/s), pressure (up to 10 bar), probe position, and probe orientation were investigated. The heat transfer coefficients increased with superficial gas velocity, and the values in the center of the column were 9–16% greater than those near the wall region under atmospheric pressure (1 bar). With the increase in pressure, the heat transfer coefficients decreased due to combined effects of bubble size decreasing, gas holdup increasing, and bubble number increasing. The heat transfer coefficients at 10 bar were about 6–17% lower than those at 1 bar for the studied conditions, where the radial profile of the heat transfer coefficients became flat with increasing pressure. The orientation of the probe qualitatively indicated the flow direction in different radial positions of the column.

Keywords: Bubble column; Heat transfer coefficient; Flow regime

1. Introduction

Bubble column and slurry bubble column reactors are widely employed in petrochemical, chemical, and biochemical processes due to their easy installation, easy operation, and high heat and mass transfer rates caused by strong gas–liquid interactions. These reactors are operated under high pressure in many industrial applications, such as heavy oil upgrading, Fischer–Tropsch synthesis, and methanol synthesis. A number of studies have been performed on the heat transfer coefficient in bubble columns. However, heat transfer coefficient studies in high-pressure bubble columns are scarce. Table 1 summarizes recent reported studies in both bubble and slurry bubble columns.

In the previous studies in these columns, generally there are two ways of obtaining the heat transfer coefficient. One of them is calculating the heat transfer coefficient based on measurement of the energy input from the heated source to the bulk media and the temperature difference between them (Baker et al., 1978; Hikita et al., 1981; Deckwer et al., 1980; Kang et al., 1985; Saxena, 1989; Cho et al., 2002). In this case, the following equation was used (Deckwer et al., 1980):

$$h = \frac{iU}{A\Delta T}, \tag{1}$$

where h is the heat transfer coefficient (kW/(m^2 K)), i is electric current (A), U is voltage (V), A is the heat transfer area (m^2) and ΔT the temperature difference between the heat source and the bulk media (K).

In applying this methodology, error in the calculation of heat flux based on the energy input is inevitable, because the heat loss in heating up all the surrounding materials, including the connecting fittings and/or column wall, was also counted into the heat transferred from the heat source to the bulk flow.

In recent years, heat flux measurement technology has progressed, and led to a second method. In this method the heat flux from the heat source to the bulk media is directly measured, and taken together with the measurement of the temperature difference between them, the heat transfer coefficient can be acquired in a more accurate way (Kumar et al., 1992; Luo et al., 1997; Li and Prakash, 1997, 2001, 2002; Yang et al., 2000; Kantarci et al., 2005). For this method, the following equation is used (Li and Prakash, 1997):

$$h_i = \frac{q_i}{\Delta T_i}, \quad h_{\text{ave}} = \frac{1}{n}\sum_{i=1}^{n}\frac{q_i}{\Delta T_i}, \tag{2}$$

* Corresponding author. Tel.: +1 314 935 7187; fax: +1 314 935 4832.
E-mail address: muthanna@wustl.edu (M.H. Al-Dahhan).

0009-2509/$ - see front matter © 2006 Elsevier Ltd. All rights reserved.
doi:10.1016/j.ces.2006.08.016

Table 1
Parameters in the literatures on heat transfer coefficients in bubble columns and slurry bubble columns

Researcher	System	Solids diameter (μm)	Solids loading (v.%)	Column diameter/height (m)	U_g (m/s)	Pressure (MPa)	Sparger	Correlation
Fair et al. (1962)	Air–water	No solid	–	0.46/3.2, 1.07/3.04	0.006–0.045	0.1	Sparger ring	$h_w = 8850U_g^{0.22}$
Hart (1976)	Air–water, air–ethylene	No solid	–	0.1/1.07	0.003–0.2	0.1	Single nozzle	$\frac{h_w}{\rho_L C_p U_g}\left(\frac{C_p\mu_L}{k_L}\right)^{0.6} = 0.125\left(\frac{U_g^3\rho_L}{\mu_L g}\right)^{-0.25}$
Deckwer et al. (1980)	Nitrogen–xylene, kogasin, decalin, nitrogen–paraffin–powdered Al_2O_3	5	0–16%	0.1/0.6	0.003–0.04	0.4–1.1	Sintered plate	$St = 0.1[(Re_m\ Fr\ Pr_m^2)^{-0.25}]$
Lewis et al. (1982)	Air–water, N_2–cumene, N_2–glycol	No solid	–	0.1/1.62, 0.19/2.4	0.02–0.165	0.1	Perforated plate	–
Hikita et al. (1981)	Air–water, air–1–butanol, air–sucrose methanol	No solid	–	0.29/1.5	0.050–0.34	0.1	Single nozzle	$\frac{h_w}{\rho_L C_p U_g}\left(\frac{C_p\mu_L}{k_L}\right)^{2/3} = 0.411\left(\frac{U_g\mu_L}{\sigma}\right)^{-0.851}\left(\frac{\mu_L^4 g}{\sigma\rho_L}\right)^{0.308}$
Verma (1989)	Air–water	No solid	–	0.11/1.7	0.1–0.4	0.1	Perforated plate	$\frac{h_w}{\rho_L C_p U_g} = 0.121(1-\bar{\varepsilon}_g)\left(\frac{C_p\mu_L}{k_L}\right)^{-0.5}\left(\frac{\mu_L^3\rho_L}{\mu_L g}\right)^{-0.851}$
Saxena (1989)	Air–water, air–water–magnetite	35.7–137.5	0–30%	0.11/2.25	0.015–0.333	0.1	Porous plate	$h_{w,\max} = 0.12\left(\frac{g^2\rho_m}{\mu_m}\right)^{1/6}\left(\frac{\rho_m-\rho_g}{\rho_m}\right)^{1/3}(k_m\rho_m C_{pm})^{1/2}$
Schlüter et al. (1995)	Air–water, air–propylene	No solid	–	0.29/4.27	0.01–0.65	0.1	Sieve tray	–
Li and Prakash (1997, 2001, 2002)	Air–water–glass beads	35	0–40%	0.28/2.4	0.05–0.35	0.1	Six-arm distributor	–
Yang et al. (2000)	Nitrogen–Paratherm NF heat transfer fluid–glass beads	53	0–35%	0.10/1.37	0.01–0.20	0.1–4.2	Perforated plate	$St = 0.037\left[(Re_m\ Fr\ Pr_m^{1.87})\left(\frac{\varepsilon_g}{1-\varepsilon_g}\right)\right]^{-0.22}$
Cho et al. (2002)	Air–viscous liquid	No solid	–	0.152/2.5	0.02–0.12	0.1–0.6	Perforated plate	–
Kantarci et al. (2005)	Air–water–yeast, air–water–cell	10, 0.2–0.7	0–0.4%	0.17/0.6	0.03–0.20	0.1	Six-arm distributor	$St = A(ReFr)^B\ Pr^C\left(\frac{x}{H}\right)^D\left(\frac{r}{R}\right)^E$

Note: C_p, heat capacity of liquid, J/(kg K); g, gravitational acceleration, m/s^2; $h_{w,\max}$, maximum heat-transfer coefficient, W/(m^2 K); U_g, superficial gas velocity, m/s; ε_g, gas holdup; ρ_g gas density, kg/m^3; σ, surface tension, N/m; C_{pm}, heat capacity of liquid–solid suspension, J/(kg K); h_w, time-averaged heat-transfer coefficient, W/(m^2 K); k_m, thermal conductivity of liquid–solid suspension W/(m K); Re_m, Reynolds number based on slurry properties; μ_m, viscosity of liquid–solid suspension, Pa s; ρ_m, density of liquid–solid suspension, kg/m^3; Fr, Froude number; k_l, thermal conductivity of liquid, W/(m K); Pr_m, Prandtl number based on slurry properties; St, Stanton number; μ_L, liquid viscosity, Pa s; ρ_L, liquid density, kg/m^3.

where h_i is the instantaneous local heat transfer coefficient (kW/(m^2 K)), q_i is the heat flux across the sensor (kW/(m^2)), ΔT_i is the instantaneous temperature difference between the heat source and the bulk (K), h_{ave} is the time averaged heat transfer coefficient (kW/(m^2 K)) and n is the total number of the samples.

In the reported studies, many parameters can affect the heat transfer in bubble/slurry bubble columns. It has been reported that the heat transfer coefficient increases with superficial gas velocity, heat capacity, and thermal conductivity of the liquid. However, it decreases with an increase in the viscosity of the liquid in gas–liquid or gas–liquid–solid systems (Deckwer et al., 1980; Saxena, 1989; Saxena et al., 1990a,b, 1991; Li and Prakash, 1997; Yang et al., 2000).

Pressure has a significant effect on the hydrodynamics and bubble dynamics (especially the bubble size) in bubble/slurry bubble columns (Luo et al., 1999). There are only a few studies about heat transfer coefficient in high-pressure reactors (Deckwer et al., 1980; Luo et al., 1997; Yang et al., 2000), an area that needs further evaluation. Deckwer et al. (1980) investigated the heat transfer coefficient from an immersed heat source to the surrounding media in a system prevailing in the Fischer–Tropsch slurry process ($P = 0.1$–1.6 MPa, $T = 143$–270 °C). However, the effect of pressure on heat transfer coefficient was not reported in their manuscript and cannot be realized by their results. By introducing the surface renewal model and Kolmogoroff theory of isotropic turbulence into their heat transfer coefficient study, they also developed a correlation to predict the heat transfer coefficient at low superficial gas velocity ($U_g < 10$ cm/s). Unfortunately, the effect of pressure was also ignored in their correlation. Luo et al. (1997) reported that at a given gas and liquid velocity in a three phase fluidized bed the heat transfer coefficient between an immersed surface and the bed increases to a maximum at a pressure of 6–8 MPa and then decreases with a further increase in pressure. Yang et al. (2000) investigated the effect of pressure on the local heat transfer coefficient in the center of a slurry bubble column. They found that the heat transfer coefficient decreases with an increase in pressure. However, all of these reported heat transfer coefficient measurements under high pressure were carried out in small diameter columns (less than 11 cm). Whereas, according to Wilkinson et al. (1992), the inner diameter of the bubble column should be equal or larger than 15 cm to avoid wall effect.

So far, there have been very limited reports on the radial profile of the heat transfer coefficients in bubble columns and slurry bubble columns (Li and Prakash, 1997; Kantarci et al., 2005). All of the provided radial profiles were under atmospheric pressure, and there is no reported information about the radial profile of the heat transfer coefficient under high pressure.

Therefore, the focus of this study is to investigate the effects of pressure, high superficial gas velocity, and orientation of the probe on the heat transfer coefficient and its radial profile in a 0.16 m diameter air–water bubble column.

2. Experiments

The experiments were performed in a 0.16 m diameter and 2.50 m high stainless steel bubble column, as shown in Fig. 1. Tap water was the liquid phase, and compressed air was the gas phase. Compressed air was supplied from two compressors connected in parallel, after it passed through a dryer and several air filter units. The flow rate of the filtered dry air was adjusted by a pressure regulator and rotameter system, consisting of four rotameters of increasing range connected in parallel. The superficial gas velocity varied from 0.03 to 0.30 m/s. Air was introduced into the column through a perforated plate gas distributor with 163 holes, and the open area ratio of the distributor was 1.09%. During the experiments the dynamic liquid height

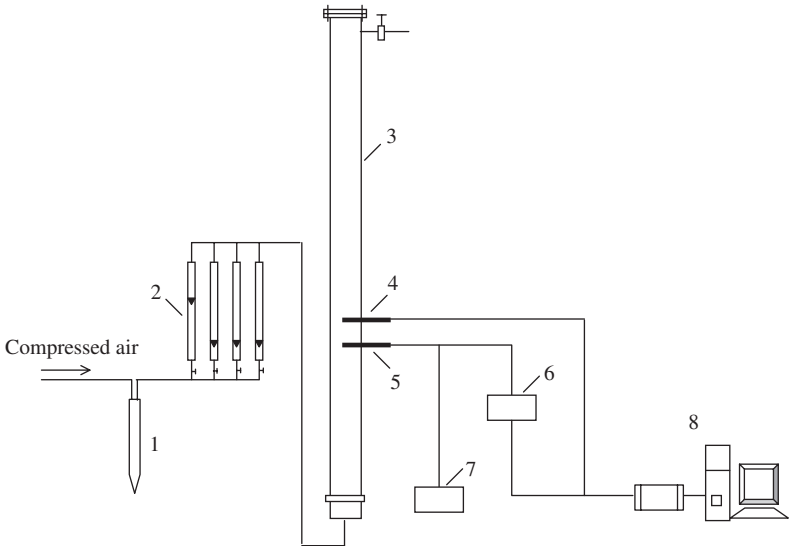

Fig. 1. Schematic of the heat transfer measurement setup: 1, filter; 2, rotameters; 3, high pressure bubble column; 4, heat transfer probe; 5, thermocouple probe; 6, amplifier; 7, DC power; 8, DAQ system.

was maintained at around 1.80 m by varying the static height at each studied condition. It was found that the range of static height variation does not affect the column hydrodynamics at the conditions studied. A thermocouple probe, which contained three thermocouples (Omega TMTSS-125U-12), was used to measure the bulk temperature of the media in the column adjacent to the heat transfer probe. The heat transfer probe (Fig. 2), manufactured at Washington University, was a modified version of the probe developed by Li and Prakash (1997). The diameter and the length of the brass shell are 11.4 and 38 mm, respectively. The heat flux sensor (11 mm × 14 mm × 0.08 mm) used on the probe is from RDF Corporation (No. 20453-1), and measures both the local heat flux and the surface temperature of the probe simultaneously. The response time of the sensor (as claimed by the manufacturer) is 0.02 s. During the experiments, the heat transfer probe was horizontally installed in the fully developed region of the bubble column, with an axial height (measured from the sparger to the heat flux sensor) to column diameter ratio (Z/D) equals to 5.1. This height was selected because it had previously been used in measuring time averaged cross-sectional gas holdup distribution using gamma ray computed tomography (CT) in the same column (Ong, 2003; Radoš, 2002).

As shown in Fig. 2, the heat flux sensor was attached to the brass shell on the outer surface, and the direction of the sensor indicated the probe orientation. At most experimental conditions, the probe was set to be lateral (see Fig. 6 for schematic lateral position) because the surfaces of heat transfer elements (e.g., bundles of vertical tubes) are oriented laterally to the flow field, as opposed to upward and downward orientation. However, the orientation effect of the probe was investigated as well. Since the measured signals of the heat flux are in the range of microvolts, they were amplified before being received by the data acquisition system. After being amplified, the heat flux signals, together with the signals from the thermocouples, were sampled at 50 Hz for more than 40 s. Since the heat flux, the temperature of the probe surface, and the bulk media temperature could be directly measured, the local instantaneous heat transfer coefficient and local averaged heat transfer coefficient could be estimated as follows:

$$h_i = \frac{q_i}{T_{si} - T_{bi}}, \tag{3}$$

$$h_w = \frac{1}{n}\sum_{i=1}^{n} \frac{q_i}{T_{si} - T_{bi}}, \tag{4}$$

where h_i is the instantaneous local heat transfer coefficient (kW/(m^2 K)), q_i the instantaneous heat flux across the sensor (kW/(m^2)), T_{bi} the instantaneous bulk temperature of the media (K), T_{si} the instantaneous surface temperature of the probe (K), h_w the time averaged heat transfer coefficient (kW/(m^2 K)), and n the total number of the samples.

3. Results and discussion

3.1. Effect of superficial gas velocity

The effect of the superficial gas velocity on the local averaged heat transfer coefficient in the center region ($r/R = 0 - r$: radial position of the sensor, R: column radius.) and in the wall region ($r/R = 0.9$) of the column is shown in Fig. 3. Both the heat transfer coefficients in the center region and those in the wall region increased with the superficial gas velocity, and the increase became smaller at higher superficial gas velocities.

According to Kumar et al. (1992), the local heat transfer coefficient has a direct connection to the bubble size: it increases with an increase in bubbles size, because large bubbles can create strong vortices and intense mixing in the wake region. It is also reported that there are three flow regimes (Fig. 4) with the increase in the superficial gas velocity in a bubble column (Chen et al., 1994). Hence, at low superficial gas velocities, the heat transfer coefficients are relatively small because of the small bubble size in the bubbly flow regime. With an increase

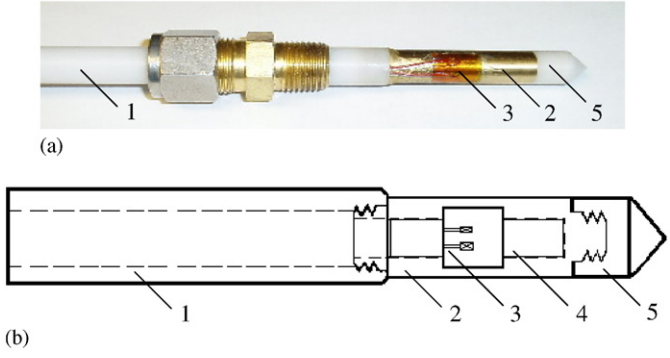

Fig. 2. (a) Picture of the heat transfer measurement probe. (b) Schematic diagram of heat transfer probe. 1, Teflon tube; 2, brass shell; 3, heat flux sensor; 4, heater; 5, Teflon cap.

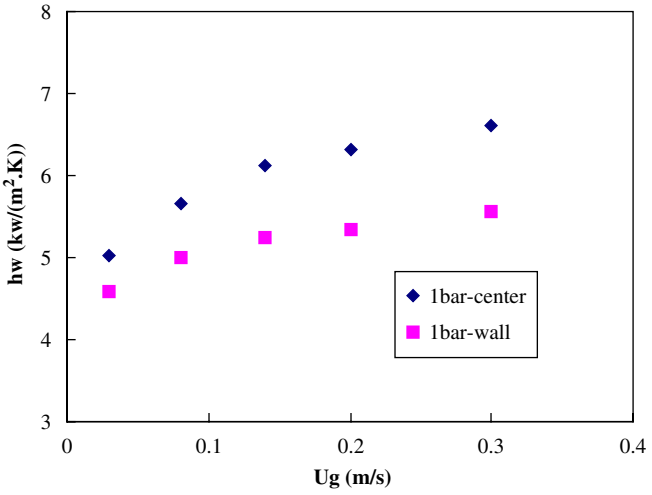

Fig. 3. The effect of superficial gas velocity and probe position on heat transfer coefficients in the fully developed region of a bubble column (pressure=1 bar).

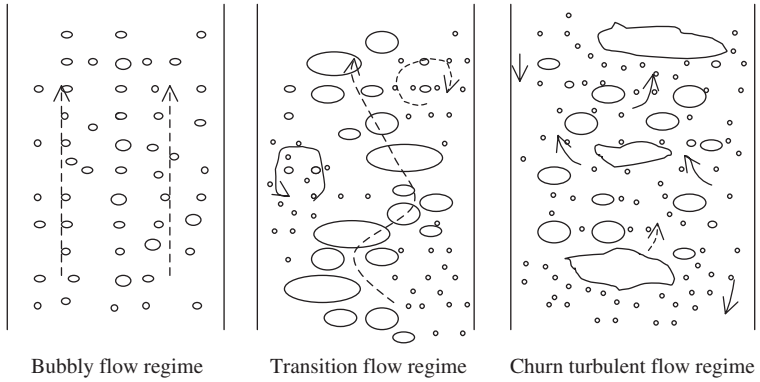

Fig. 4. Flow regimes in a 3-D bubble column (Chen et al., 1994).

of superficial gas velocity, the heat transfer coefficients increase due to the increase of bubble sizes and their number and passage frequency in the transition (vertical–spiral) and churn turbulent flow regimes. In the churn turbulent flow regime, the magnitude of the increase slows down, since bubble coalescence and breakup come to a balance at a certain velocity as mentioned earlier (Luo et al., 1999).

In Fig. 3, the heat transfer coefficients in the center are larger than those in the wall region, and the amount varies from 9% to 16% with the increase in superficial gas velocity. The differences at low superficial gas velocities are relatively small, but at high superficial gas velocities the differences become larger. It reflects that bubbles with relatively small diameters are uniformly distributed across the column radius at low superficial gas velocities. With a further increase in superficial gas velocity, large bubbles are formed, and most of them rise through the core region of the column at high bubble frequency, causing high gas holdup in the center region. However most small bubbles move in the wall region of the column, where the liquid/slurry flow is downward (Ong, 2003; Radoš, 2002), at low bubble frequency causing low gas holdup (Xue, 2004).

Fig. 5 shows a comparison between the heat transfer coefficients measured in this work in the center of an air–water bubble column at the fully developed region under atmospheric pressure and the reported values at similar operating conditions. Since Schlüter et al. (1995) did not explain the experimental method used, it is hard to evaluate why their results are larger than the measured values in this work. Hikita et al. (1981) measured the heat transfer coefficients between the column wall and the gas–liquid dispersions in the bubble column, and they directly used the energy input to calculate the heat transfer coefficient. And hence, their results are not considered in the following comparison. The results in this work and those reported by Verma (1989), Saxena et al. (1990a), and Li and Prakash (1997) were obtained using immersed cylindrical heaters. As reported by Saxena et al. (1990b), column diameter can affect the heat transfer coefficient, and the heat transfer coefficient increases with the increase in the column diameter in a bubble column without internals. The results shown in Fig. 5 are consistent with this finding particularly at high superficial gas

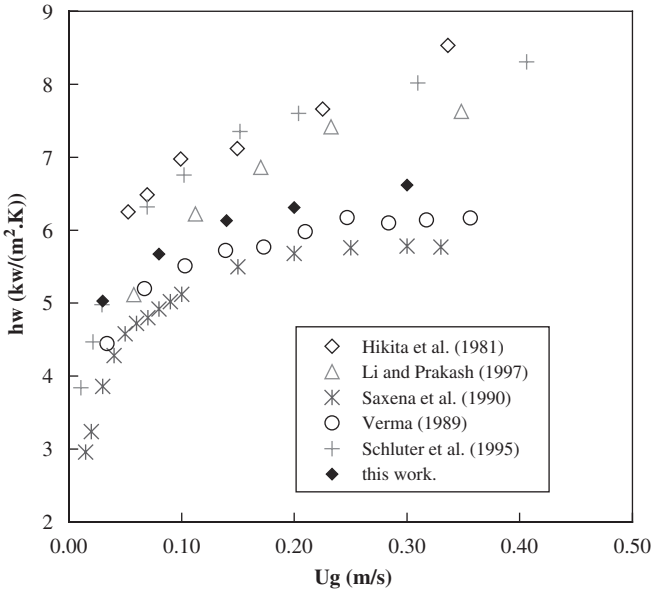

Fig. 5. Comparison of the heat transfer coefficients in this work with the reported data in the center of an air–water bubble column at the fully developed region (pressure = 1 bar).

velocities, where the column diameter used by Verma (1989) and Saxena (1989) was 0.108 m, while the column diameter used in this work was 0.16 m, and the column diameter used by Li and Prakash (1997) was 0.28 m.

3.2. Effect of pressure

Fig. 6 shows the effect of pressure on the heat transfer coefficient in a bubble column. With the change of pressure from 1 to 10 bar, the heat transfer coefficients decreased in both the center and the wall regions of the column. The decreases of the heat transfer coefficients in the center of the column varied from 17% to 8% and the decreases in the wall region varied from 14% to 6%, at an increasing superficial gas velocity.

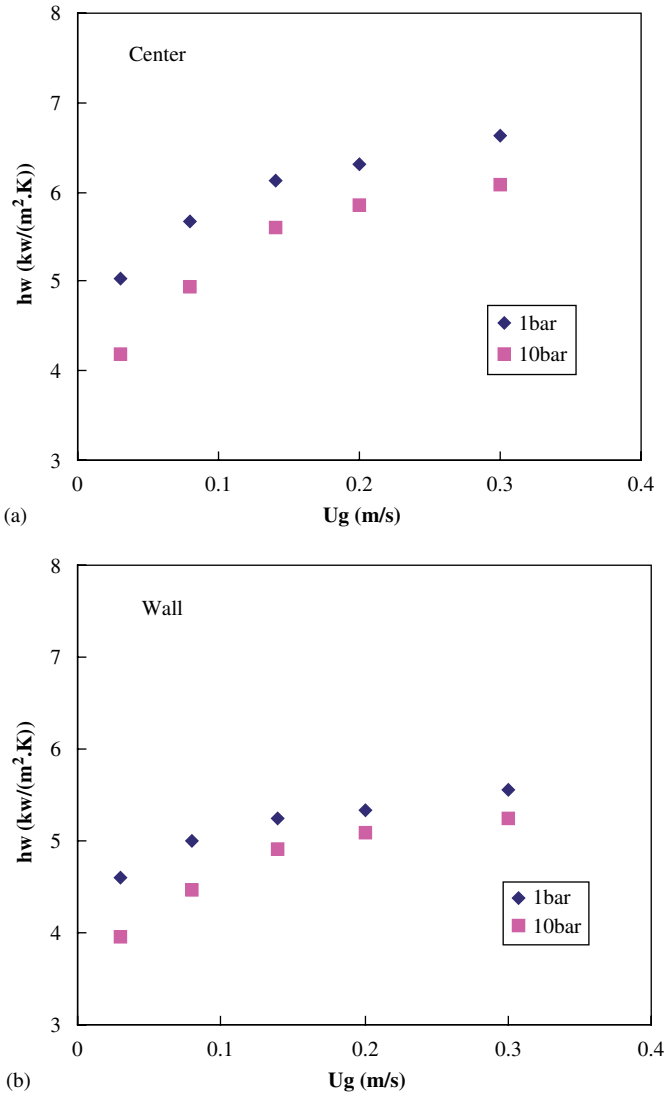

Fig. 6. Effect of pressure on heat transfer coefficients in the fully developed region of a bubble column: (a) in the center of the column ($r/R = 0$), (b) near the wall of the column ($r/R = 0.9$).

Pressure can affect the liquid properties such as density, viscosity and surface tension, but these effects were relatively small under the experimental conditions of this work. With the increase in the pressure the gas density increases, which causes the decrease of the initial bubble size from the sparger and the increase of bubble breakup rate (Luo et al., 1999). Due to these effects, pressure decreases the bubble size, and narrows the range of bubble size distribution. Hence, the decrease in the heat transfer coefficient at an elevated pressure is the combined effect of all the related parameters mentioned above, and bubble size is the dominant factor at the studied experimental conditions.

In Fig. 6, the decreases of the heat transfer coefficients at low superficial gas velocities were larger than those at high superficial gas velocities. As mentioned above, the overall decrease trend of the heat transfer coefficient with increasing pressure is mainly due to the decrease of bubble size. However, the bubble frequency and bubble number increase with elevated pressure, which enhance the liquid circulation in the bubble column. At low gas velocity, although the total number of bubbles increases under high pressure, the liquid circulation does not change much because bubble coalescence and break up are insignificant in this bubbly regime. At high superficial gas velocity, more large bubbles are formed in the transition flow regime and churn turbulent flow regime. Even though the average size at high pressure is smaller than that under atmospheric pressure, the enhanced bubble frequency and increased bubble number under high pressure cause intense interaction between bubble–bubble, bubble–liquid, liquid–wall, and liquid–probe surface. Such enhanced interactions due to pressure decrease the thickness of the contact film between the probe and the bulk and then increase the heat transfer coefficient to some extent. It is noteworthy that these enhancements on heat transfer coefficient due to increasing bubble number and bubble frequency with increasing pressure are not as strong as the effect of the bubble size reduction (Yang et al., 2000). Hence, at high superficial gas velocities (churn turbulent flow regime) the differences in the heat transfer coefficient between low pressure and high pressure become smaller as compared to low range superficial gas velocities (bubbly flow regime).

3.3. Identification of flow direction by the heat transfer probe

Flow direction is important in understanding the flow structure in the bubble columns and slurry bubble columns. Using the measurement of the heat transfer coefficients (shown in Fig. 7) at different orientations of the sensor on the probe, the flow direction can be qualitatively identified (upward or downward). In Fig. 7a, in the center of the column, the heat transfer coefficient in the downward direction was the largest, which indicates an enhanced upward gas–liquid flow in the center of the column. On the other hand, as shown in Fig. 7b, an enhanced downward flow in the wall region of the column can be indicated. These observations are consistent with the findings reported by Li and Prakash (2002). Such a method can also be utilized to qualitatively indicate the flow directions at different regions in large bubble column reactors equipped with internals, in which the hydrodynamics is much more complex and the flow direction could be harder to predict than the bubble column without internal.

3.4. Radial profile of the heat transfer coefficient

For the first time the radial profiles of the heat transfer coefficients under high pressure were provided in a bubble column. Fig. 8a shows radial profiles of heat transfer coefficients in an air–water bubble column at several different superficial gas velocities under both atmospheric pressure and high pressure. To learn how the radial profile changes with the superficial gas velocity and pressure, the heat transfer coefficients were normalized by taking the ratio of the heat transfer coefficients at different radial positions to the values obtained in the center of the column at the same operating conditions.

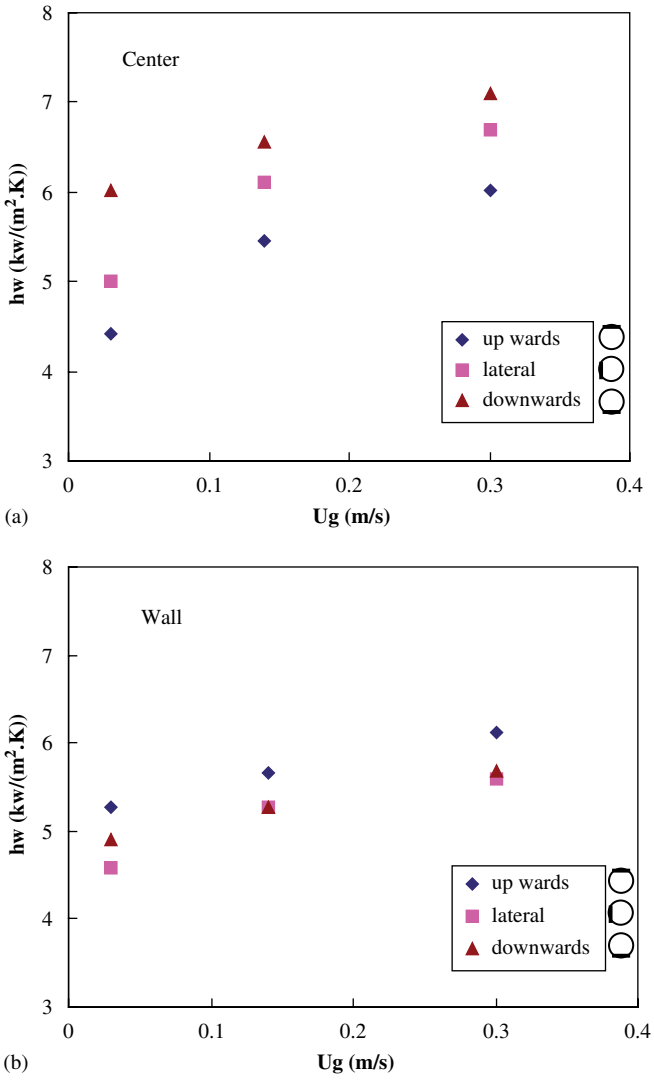

Fig. 7. Effect of probe orientation on heat transfer coefficients in the fully developed region of a bubble column (pressure = 1 bar): (a) in the center of the column ($r/R = 0$), (b) near the wall of the column ($r/R = 0.9$).

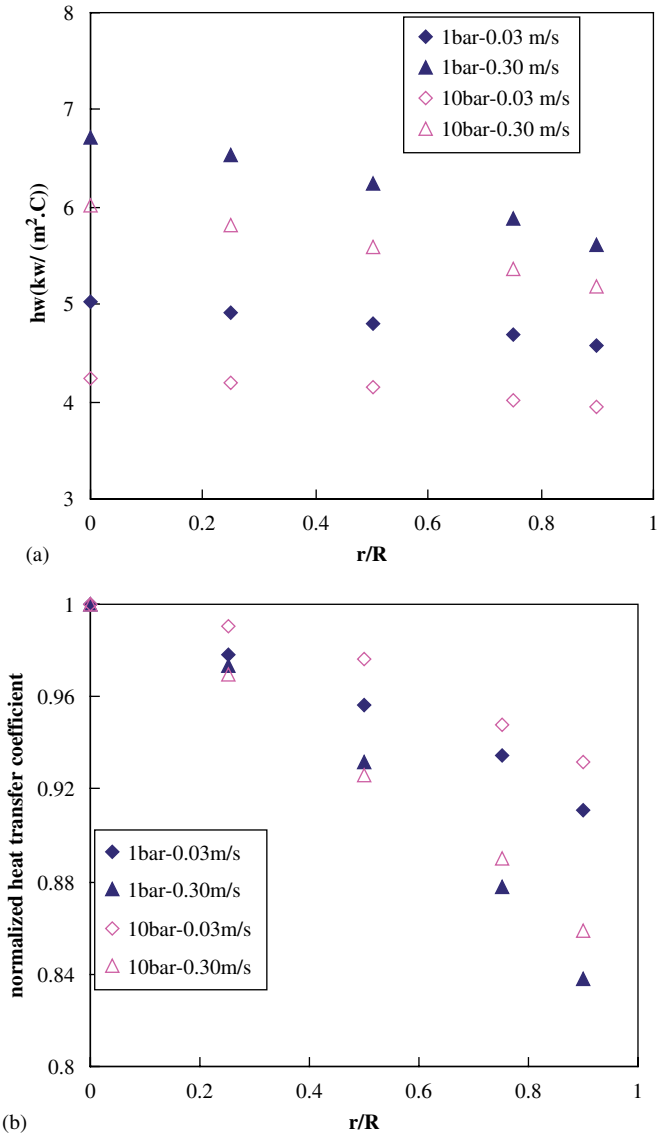

Fig. 8. Radial profile of heat transfer coefficient in the fully developed region of a bubble column: (a) original measured heat transfer coefficients, (b) normalized heat transfer coefficient.

Fig. 8b shows the profile of the normalized heat transfer coefficients. The radial profiles of the heat transfer coefficients at low superficial gas velocities had lower gradient than those at high superficial gas velocities under both atmospheric pressure and high pressure in the bubble column. At low superficial gas velocities the bubble sizes at different radial positions are similar, and there is no significant bubble break up and coalescence. However, at high superficial gas velocities, most large bubbles form in the core of the column and rise at high bubble frequency, which causes the uneven distribution of bubble size across the radial direction (Xue, 2004).

It can also be seen that at the same superficial gas velocity the radial profiles of the heat transfer coefficients became flatter with increasing pressure. It is known that pressure has an important effect on bubble size, bubble distribution, and gas holdup (Luo et al., 1999). With increasing pressure, the average bubble size decreases, and the range of bubble size distribution narrows, which cause lower gradient of the radial profiles of both the gas holdup (Ong, 2003; Radoš, 2002) and heat transfer coefficient under high pressure.

4. Summary

Heat transfer coefficient measurements were conducted in a 0.16 m diameter air–water high-pressure bubble column. The effects of superficial gas velocity, pressure, probe orientation, and radial position on heat transfer coefficients were investigated. The heat transfer coefficient increased with superficial gas velocity, and at high velocities the increase became smaller. At the same operating conditions, the heat transfer coefficient in the center of the column was larger than that near the wall region, and the differences at low superficial gas velocities were smaller than those at high superficial gas velocities. With increased pressure, the heat transfer coefficient decreased,

whereas, the differences at low superficial gas velocities were larger than those at high superficial gas velocities. The orientation of the probe reflects the flow direction in a different region of the column. For the first time, the radial profiles of the heat transfer coefficient under high pressure was investigated, and it was found that the radial profiles of heat transfer coefficients become flatter at high pressure due to decreasing bubble size and shrinking bubble size distribution with an increase in pressure.

Acknowledgments

This project was supported by the high-pressure slurry bubble column consortium, including Conocophillips (USA), Enitechnology (Italy), Sasol (South Africa), and Statoil (Norway).

References

Baker, C.G.J., Armstrong, E.R., Bergougnou, M.A., 1978. Heat transfer in three-phase fluidized beds. Powder Technology 21, 195–204.

Chen, R.C., Reese, J., Fan, L.-S., 1994. Flow structure in a three-dimensional bubble column and three-phase fluidized bed. A.I.Ch.E. Journal 40, 1093–1104.

Cho, Y.J., Woo, K.J., Kang, Y., Kim, S.D., 2002. Dynamic characteristics of heat transfer coefficient in pressurized bubble columns with viscous liquid medium. Chemical Engineering and Process 41, 699–706.

Deckwer, W.-D., Louisi, Y., Zaidi, A., Ralek, M., 1980. Hydrodynamic properties of the Fischer–Tropsch slurry process. Industrial and Engineering Chemistry Research 19, 699–708.

Fair, J.R., Lambright, A.J., Anderson, J.W., 1962. Heat transfer and gas holdup in a sparged contactor. Industrial and Engineering Chemistry, Process Design and Development 1, 33–36.

Hart, W.F., 1976. Heat transfer in bubble-agitated systems. A general correlation. Industrial and Engineering Chemistry Research 15, 109–114.

Hikita, H., Asal, S., Kikukawa, H., Zaike, T., Ohue, M., 1981. Heat transfer coefficient in bubble columns. Industrial and Engineering Chemistry, Process Design and Development 20, 540–545.

Kang, Y., Suh, I.S., Kim, S.D., 1985. Heat transfer characteristics of three phase fluidized beds. Chemical Engineering Communications 34, 1–13.

Kantarci, N., Ulgen, K.O., Borak, F., 2005. A study on hydrodynamics and heat transfer in a bubble column reactor with yeast and bacterial cell suspensions. The Canadian Journal of Chemical Engineering 83, 764–773.

Kumar, S., Kusakabe, K., Raghunathan, K., Fan, L.-S., 1992. Mechanism of heat transfer in bubbly liquid and liquid–solid systems: single bubble injection. A.I.Ch.E. Journal 38, 733–741.

Lewis, D.A., Field, R.W., Xavier, A.M., Edwards, D., 1982. Heat transfer in bubble columns. Transactions of the Institution of Chemical Engineers 60, 40–47.

Li, H., Prakash, A., 1997. Heat transfer and hydrodynamics in a three-phase slurry bubble column. Industrial and Engineering Chemistry Research 36, 4688–4694.

Li, H., Prakash, A., 2001. Survey of heat transfer mechanisms in a slurry bubble column. The Canadian Journal of Chemical Engineering 79, 717–725.

Li, H., Prakash, A., 2002. Analysis of flow patterns in bubble and slurry bubble columns based on local heat transfer measurements. Chemical Engineering Journal 86, 269–276.

Luo, X., Jiang, P., Fan, L.-S., 1997. High-pressure three-phase fluidization: hydrodynamics and heat transfer. A.I.Ch.E. Journal 43, 2432–2444.

Luo, X., Lee, D.J., Lau, R., Yang, G.Q., Fan, L.-S., 1999. Maximum stable bubble size and gas hold up in high-pressure slurry bubble column. A.I.Ch.E. Journal 45, 665–680.

Ong, B.C., 2003. Experimental investigation of bubble column hydrodynamics: effect of elevated pressure and superficial gas velocity. Ph.D. Thesis, Washington University in Saint Louis.

Radoš, N., 2002. Slurry bubble column hydrodynamics: experimentation and modeling. Ph.D. Thesis, Washington University in Saint Louis.

Saxena, S.C., 1989. Heat transfer from a cylindrical probe immersed in a bubble column. Chemical Engineering Journal 41, 25–39.

Saxena, S.C., Rao, N.S., Saxena, A.C., 1990a. Heat transfer from a cylindrical probe immersed in a three-phase slurry bubble column. Chemical Engineering Journal 44, 141–156.

Saxena, S.C., Rao, N.S., Saxena, A.C., 1990b. Heat-transfer and gas-holdup studies in a bubble column: air–water–glass bead system. Chemical Engineering Communications 96, 31–55.

Saxena, S.C., Rao, N.S., Yousuf, M., 1991. Heat-transfer and hydrodynamic investigations conducted in a bubble column with powders of small particles and viscous liquid. The Chemical Engineering Journal 47, 91–103.

Schlüter, S., Steiff, A., Weinspach, P.-M., 1995. Heat transfer in two- and three-phase bubble column reactors with internals. Chemical Engineering and Processing 34, 157–172.

Verma, A.K., 1989. Heat transfer mechanism in bubble column. Chemical Engineering Journal 42, 205–208.

Wilkinson, P.M., Spek, A.P., Laurent, D.L., 1992. Design parameters estimation for scale-up of high-pressure bubble columns. A.I.Ch.E. Journal 38, 544–554.

Xue, J., 2004. Bubble velocity, size and interfacial area measurements in bubble columns. Ph.D. Thesis, Washington University in Saint Louis.

Yang, G.Q., Luo, X., Lau, R., Fan, L.-S., 2000. Heat transfer characteristics in slurry bubble columns at elevated pressures and temperatures. Industrial and Engineering Chemistry Research 39, 2568–2577.